Low-Z-Impurity Transport Coefficients at ASDEX Upgrade

S de Peña Hempel, R Dux, A Kallenbach, H Meister, ASDEX Upgrade Team
MPI für Plasmaphysik, EURATOM Association, D-85748 Garching, Germany

Introduction

Impurity transport studies were conducted in ASDEX Upgrade by injecting short puffs of *He* or *Ne* gas during an otherwise steady-state phase of a discharge. Charge exchange recombination spectroscopy (CXRS) measurements were used to monitor the temporal evolution of the radial impurity profiles subsequent to these puffs. Following the temporal evolution of the profiles the diffusion coefficient D and the convective velocity v were determined. The radial profiles and parametric dependences of the particle transport coefficients are analysed in different confinement regimes. Furthermore the dynamic behaviour of the transport during sawtooth-free discharge periods and ELMs is studied and compared with model predictions.

Determination of local transport coefficients

Spatially and temporally resolved impurity densities in the core plasma of the ASDEX Upgrade tokamak are obtained in neutral beam heated discharges from CXRS measurements with a set of 14 viewing lines of sight. The transport coefficients are determined by first inferring the particle flux Γ from the measured temporal evolution of the impurity density profile by inverting the continuity equation in the source free region. The assumption of zero sources is only accurate inward of the region of ionization at the plasma edge ($\rho_{\mathrm{pol}} < 0.8$ for *Ne* and $\rho_{\mathrm{pol}} < 0.95$ for *He*). The impurity fluxes are described by the extended Fick's Ansätz $\Gamma(r,t) = -D(r)\nabla n(r,t) + v(r)n(r,t)$ which assumes the particle flux to be made up of a diffusive flux and an unspecified convective flow which incorporates any additional terms not dependent on the density gradient. Thus, the normalized flux $\frac{\Gamma}{n}$ at a particular minor radius is an offset linear function of the density scale length $\frac{\partial n}{n}$, consistent with expectations for a trace impurity and time-independent transport coefficients. From such a curve the diffusion coefficient is determined by the absolute value of the slope of the linear regression to the data and the convective velocity by the y-intercept. To overcome the instrumental noise in the experimental data, which gives the main contribution to the uncertainty in the determination of the transport coefficients, smooth functions are used to fit the temporal evolution and radial profile.

Dependences and scaling laws for the impurity transport coefficients

Empirical scaling laws for the particle transport coefficients were determined by extending the previously described flux analysis to 74 different neutral-beam-heated L-, H- and CDH-mode discharges covering the parameter range: $1.89 < B_{\mathrm{tor}}[T] < 2.69$, $1.99 < P_{\mathrm{tot}}[MW] < 9.13$, $4.49 < \bar{n}_e[10^{19}\frac{1}{m^3}] < 11.75$ und $1.15 < m_{\mathrm{eff}}[amu] < 1.90$. The variation range in the plasma current was too narrow to examine any dependence on this parameter and so the evaluation of the scaling was restricted to discharges with $I_p = 1\,MA$. In addition the effect of possible collinearities with the magnetic field could be eluded. Furthermore, only *He* and *Ne* pulses during otherwise steady-state phases of a discharge were analysed. This was accomplished by allowing a maximal excursion of 10% in the time evolution of the line-integrated electron density, neutral injection heating power and energy confinement time.

In the plasma core region a nonlinear regression of the diffusion coefficient yields

$$D(\rho_{\rm pol}=0.2) = 0.293 \cdot B_{\rm tor}^{-0.183\pm0.082} \cdot P_{\rm tot}^{0.473\pm0.026} \cdot m_{\rm eff}^{-0.666\pm0.047} \qquad (1)$$

irrespective of the discharge confinement mode. Within the uncertainties in the determination of this scaling no significant dependence on the injected impurity species or the electron density is found. In addition, the diffusion coefficients are determined to vary roughly as the square root of the total heating power. They exhibit a marked dependence on the background plasma species and decrease with the toroidal magnetic field. Figure 1a) demonstrates the good reproduction of the measured diffusion coefficients by the scaling law of equation 1.

In the outer plasma region the inferred parameter dependencies show the same tendencies as found for the plasma core. However the errors of the exponents in this region are comparable to the exponents themselves and are therefore of no sufficient quality to determine the dependences exactly. Individual regressions for the different confinement regimes lead to similar results. In good agreement with the results of gas puff or gas modulation experiments in other machines, the diffusion coefficient for stationary plasma conditions is one or two orders of magnitude larger than the prediction of the neoclassical transport theory over the complete radial range and has a hollow radial profile.

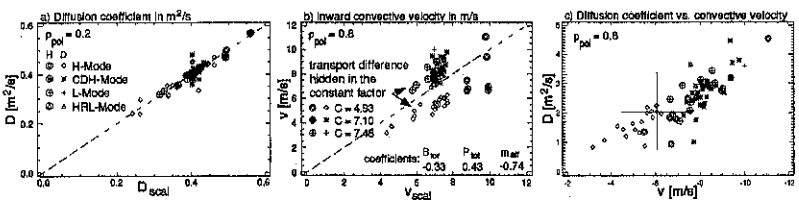

Figure 1: *a: Measured central diffusion coefficient versus the prediction of the scaling law of equation 1. b: Measured pinch velocity versus scaling law at the plasma edge. c: Inward pinch velocity versus diffusion coefficient at* $\rho_{\rm pol} = 0.8$.

The inward convective velocity on the contrary only exceeds the neoclassical value at radii larger than $\rho_{\rm pol} \sim 0.6$, where it shows a strong correlation with the diffusion coefficient (fig.1c), suggesting that a common mechanism gives rise to both transport coefficients. For $\rho_{\rm pol} \geq 0.6$ the scaling of both transport coefficients exhibits similar dependences as have been put forward for the diffusion coefficient in the core region (tabular in fig.1c), however, there is a marked influence of the confinement regime on the impurity transport behaviour. This cannot be explained by any parameter dependence and is hidden in the constant scaling factor. Due to its large relative error no parameter dependences could be inferred for the pinch velocity in the central plasma.

A comparison of the impurity transport coefficient with published results for the electron transport [1,2] points out a good agreement in the absolute magnitude and radial profile shape of the coefficients as well as a clear parallelism concerning the analyzed parametric dependencies. Further on a satisfactory correlation with the scaling laws for the energy and the angular momentum confinement time [3] is found.

Instationary accumulation phenomena in sawtooth-free discharge periods

The impurity transport coefficients in the previous paragraph were determined in saw-

toothing discharges and represent sawtooth averaged values. For instationary accumulation phenomena during sawtooth-free discharge periods the impurity transport in the plasma center shows a different behaviour. The suppression of sawteeth observed in some radiating boundary CDH-mode discharges is accompanied by the development of density peaking [4] and a slightly enhanced energy confinement. Simultaneous measurement and evaluation of the carbon and neon CXR-spectra in addition with Z_{eff}-profile measurements from the deconvolution of the line integrated bremsstrahlung background radiation shows that although these phases exhibit a central accumulation of neon and a strong peaking of the soft x-ray and Z_{eff}-profiles the carbon density profile evolution remains unchanged.

The transport analysis in these sawtooth-free discharge periods leads to a diffusion coefficient that reduces to neoclassical values for poloidal fluxes smaller than $\rho_{\text{pol}} \sim \sqrt{2}\rho_{\text{pol}}^{\text{inv}} \approx 0.65$. For larger radii the diffusivity is not affected by the sawtooth collapse. This is consistent with the picture that the sawteeth induce a strong convective particle flow inside and outside the q=1-surface. Otherwise, the measured pinch velocity is not significantly altered by this process.

A self consistent modelling of the impurity transport and radiation with the radial impurity transport code STRAHL from the given electron and impurity densities [5] shows that for discharges without sawteeth the central ($\rho_{\text{pol}} < 0.6$) transport can be described by neoclassical terms. This modelling, however, predicts also a small but not observed peaking of the carbon density. Such an inconsistency may be due to the neglected friction between the impurity species.

Dynamic transport behaviour during type I ELM's

Due to the limitations of the detection system regarding its minimal exposure and readout time, the dynamic ELM-behaviour has to be investigated by a special mapping procedure to fasten the effective temporal resolution of the CCD system. This is achieved by analysing steady state discharge periods and considering each ELM as the consequence of the repetition of the same event. Using the maxima of the characteristic H_α-signal as the indicator for each ELM a time base can be constructed, which allows the projection of the density evolution measured in such a phase (up to 200 ELM's) onto one unique event. To obtain the real temporal behaviour of the density over an ELM the mapped signal is deconvolved with the CCD-exposure function. The study of the edge transport behaviour is restricted to helium, because the described analysis is only accurate inward of the ionisation region of the observed impurity.

The ELM's are described by an enhancement of the particle diffusion coefficient from $D \approx 1\,\frac{m^2}{s}$ up to $D_{\text{max}} \approx 6\,\frac{m^2}{s}$ in combination with an outward directed convective flow with a pinch velocity in the order of $+15\,\frac{m}{s}$ (fig.2b). However, the contributing of each term to the total particle flow is ambiguous. The rise of the transport coefficients is localized in a $\sim 10\,cm$ wide layer inside the separatrix. The given error bars include the statistical uncertainity in the evaluation of the transport coefficients from the Γ_Z^{norm}–$\partial n_Z^{\text{norm}}$–plots. The density relaxation after the ELM collapse (dashed lines) is found to be well described by the same set of transport coefficients as derived from gas puff experiments (dotted lines). The pronounced decrease of v in the region outside $\rho_{\text{pol}} = 0.95$ is possibly due to not neglegible source terms in the continuity equation. The *He*-transport coefficients derived for this region should therefore be treated with care.

The transport coefficients are compared with measurements of the effective electron diffusion coefficient and heat conductivity (fig.2c). The time evolution, the absolute magnitude and the localization of the different measurements is found to be in good qualitative and

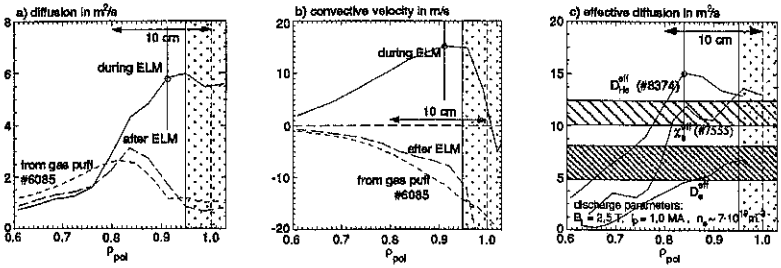

Figure 2: *Measured diffusion coefficient a) and pinch velocity b) for an ELM. c) shows a comparison of the effective He-diffusivity with values for the electron diffusion coefficient and heat conductivity.*

quantitative agreement ($D_{He}^{\text{eff}} \approx D_e^{\text{eff}} \approx \chi_e^{\text{eff}}$), suggesting that a strong link exists between thermal, electron and impurity transport during ELMs. The driving mechanism should therefore be of convective and ambipolar nature.

The predictions of model calculations based entirely on parallel particle fluxes along stochastic magnetic fields during magnetic ELM precursor activity correspond quite well to the experimental data of COMPASS-D [6] and ASDEX Upgrade [7]. The magnetic perturbation is assumed to be created by helical perturbation current filaments which are modelled to match the phase and amplitude of the ELM precursor signal measured by the Mirnov diagnostic. Subsequent field line tracing shows an ergodization between island chains and in a radial transport enhancement due to parallel particle motion along the radially excursing field lines. However the achieved good quantitative agreement between model and measurement has to be treated with care because the calculated heat conductivity is based on the transport formula of Rechester-Rosenbluth [8] which describes a conductive and non ambipolar process. This is inconsistent with the experimental results, which exhibit almost equal thermal and particle transport rates. Nevertheless, an extension of the former model including nonlinear bunching of the electrons [9] shows that the edge electron heat flux can be convective and ambipolar constrained and described by a Rechester-Rosenbluth diffusivity, but with the slow ion thermal velocity as the streaming factor $\chi_\perp^{\text{T}} = v_i \frac{\langle(\partial r)^2\rangle}{(\partial l)} \left(\frac{\omega}{k v_i}\right)^2$. The determination of the fluctuation phase velocity $u = \frac{\omega}{k}$ will be possible with the new extended magnetic coil arrangement at ASDEX Upgrade and a quantitative comparison of the modelling results to the experiment is expected.

References

[1] J O'Rourke *et al.*, Plasma Physics And Controlled Fusion 35:585–594, 1993
[2] J-L Lachambre *et al.*, Plasma Physics And Controlled Fusion 38:1943–1966, 1996
[3] H Meister, Diploma Thesis, Universität Augsburg, 1996
[4] A Kallenbach *et al.*, Plasma Physics And Controlled Fusion 38:2097–2112, 1996
[5] R Dux *et al.*, Proc. of the 23rd EPS, Kiev, I: 25–28, 1996
[6] R Buttery *et al.*, Proc. of the 22nd EPS, Bournemouth, III: 273-276, 1995
[7] H Reimerdes, IPP Report 1/300, 1996
[8] A B Rechester and M N Rosenbluth, Physical Review Letters (40)1:38–41,1978
[9] P W Terry *et al.*, Phys.Plasmas, 3(5):1999–2005,1996